

# We are IntechOpen, the world's leading publisher of Open Access books Built by scientists, for scientists

4,800

Open access books available

122,000

International authors and editors

135M

Downloads

Our authors are among the

154

Countries delivered to

TOP 1%

most cited scientists

12.2%

Contributors from top 500 universities



WEB OF SCIENCE™

Selection of our books indexed in the Book Citation Index  
in Web of Science™ Core Collection (BKCI)

Interested in publishing with us?  
Contact [book.department@intechopen.com](mailto:book.department@intechopen.com)

Numbers displayed above are based on latest data collected.  
For more information visit [www.intechopen.com](http://www.intechopen.com)



---

# Numerical Analysis of Hot Polymer-Coated Steel Pipeline Joints in Bending

---

Finian McCann, Guido Ridolfi, Erwan Karjadi,  
Harm Demmink and Helen Boyd

Additional information is available at the end of the chapter

<http://dx.doi.org/10.5772/intechopen.72262>

---

## Abstract

A numerical method to analyse the effect of the application of polymer coatings on the bending resistance of steel pipeline joints is presented. Experiments were conducted by Heerema Marine Contractors at Heriot Watt University to investigate the influence of the thickness of polymer field joint coatings and the cooldown time provided after applying the coating on the behaviour of pipeline joints when being bent during reeling operations. Temperature readings were obtained from thermocouples inside the polymer field joint coating during the application process, and pipeline ovality measurements were taken during mechanical testing. Thermal modelling of the coating application procedure was developed using COMSOL Multiphysics; this model was validated against the thermocouple readings, while a mechanical model simulating the pipe being bent to a reel was developed in Abaqus finite element modelling software. The temperature outputs, areas of stress concentration and pipe ovalities obtained from the experiments are shown to be predicted accurately by the numerical models. Upon successful validation of the numerical models, a parametric study was conducted assessing the influence of field joint coating thickness and cooldown times, in order to find an optimal design solution to reduce the cooldown time required prior to bending the pipe without buckling.

**Keywords:** nonlinear mechanics, polymers, reel-lay method, steel pipelines, subsea engineering, thermo-mechanical modelling

---

## 1. Introduction

In the field of subsea engineering, the reel-lay method offers logistical and technical advantages over alternative pipe laying methods such as J-lay as S-lay [1]. A considerable length of pipeline is fabricated and coated onshore from pipe segments, which are welded together to form

---

individual stalks, as shown in **Figure 1a**. The stalks are spooled continuously onto a reel situated on a barge (see **Figure 1b** and **c**) docked at an onshore production facility, with tie-in welds performed to join consecutive stalks together to form a contiguous pipeline typically numerous kilometres in length. The barge then transports the loaded reel out to a construction vessel offshore, such as Heerema Marine Contractors' deepwater construction vessel DCV *Aegir* (see **Figure 2a**), where it is installed onto the vessel. The pipe is fed over the aligner wheel on the lay tower, through a straightener and through the moonpool in the deck of the vessel, then subsequently unspooled and laid on the seabed (see **Figure 2b**). In the case of the *Aegir*, logistical advantages are offered by three reels being available. While a reel is being unspooled onboard the vessel and pipe being laid offshore, another reel can be loaded with another pipeline back onshore, with yet another reel in transit either to or from the vessel. Compared to the J-lay method where the pipeline is fabricated onboard the vessel by welding successive 50 to 75 m-long segments together, the onshore fabrication process is far less susceptible to the suspension of operations due to adverse weather conditions, and the overall process of unspooling and laying the pipe is considerably quicker and thus also less likely to be affected by scheduling or weather delays [2].

In order to provide mechanical protection, corrosion protection and thermal insulation for the product conveyed within, the steel pipes are coated with a polymer linepipe coating. In order to maintain the temperature of production fluids during operation and shutdown conditions, thicker coatings have had to be employed to enhance the thermal performance of the pipeline solution [3]. There are considerable challenges inherent to installing pipes with such thick coatings; it has been found previously [4] that combinations of coating thickness, pipe wall thickness and mismatch in material properties across a field joint can result in buckling. These challenges are especially present when employing the reel-lay method where the pipeline, welds and coatings typically undergo a number of bending events during fabrication, spooling, unspooling and eventual touchdown on the seabed. Previous projects have seen Heerema successfully reel and lay pipelines with a 53 mm-thick multiple layer polypropylene (MLPP) coating; the

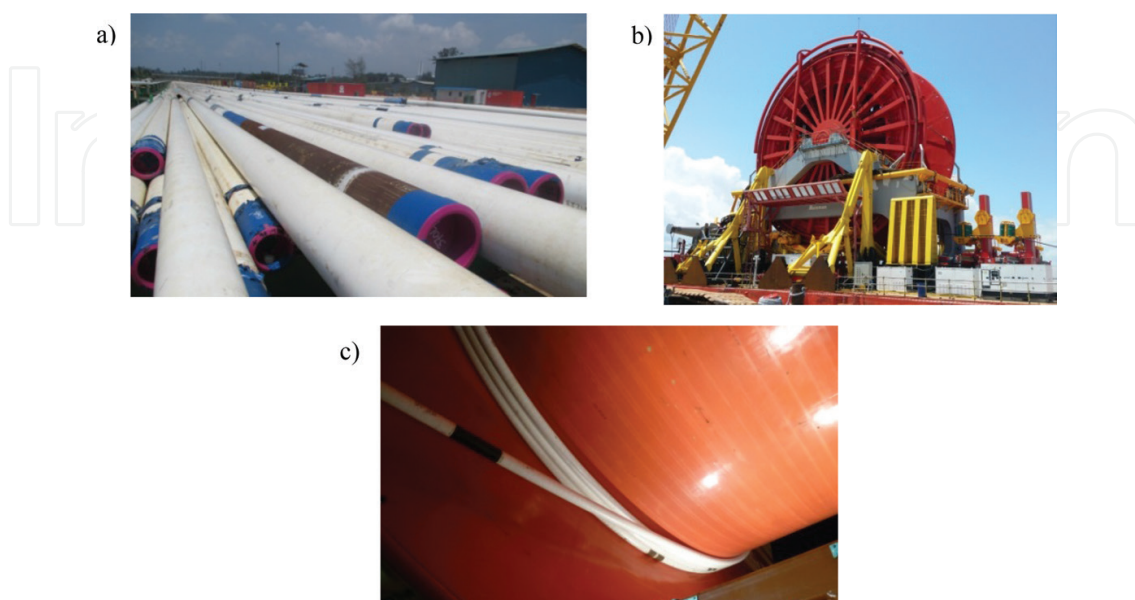


**Figure 1.** (a) Stalks prepared onsite; (b) empty reel drum onboard a barge; (c) reeling of pipeline stalks.

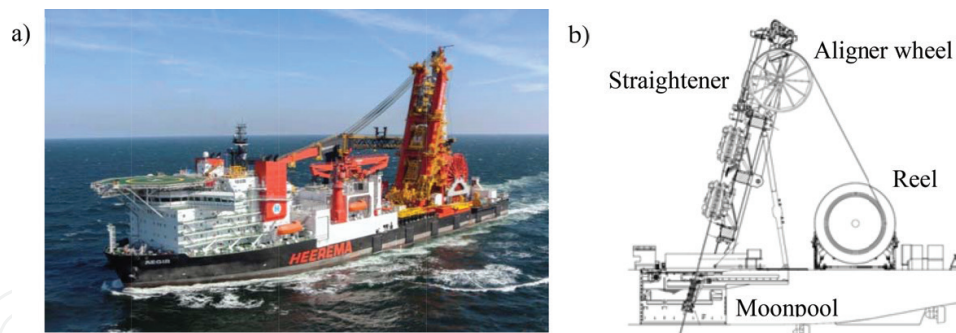


**Figure 2.** (a) DCV *Aegir*, owned and operated by Heerema Marine Contractors, capable of reel-lay and J-lay; (b) schematic of reel-lay system onboard the *Aegir*.

impetus for the investigation described in the current chapter was to ascertain whether this capacity could be extended to considerably thicker coating systems. Extending the envelope to encompass these coating solutions would allow Heerema to employ the reel-lay method to lay pipeline in ever more challenging environments and greater water depths. The current chapter focuses on pipelines with a 9LPP coating with an overall thickness of 100 mm.

In order not to damage the polymer coating when welding pipe segments together, it is necessary to cut back the coating approximately 300 mm either side of the weld, typically with a 30° chamfer to provide a smooth transition between the linepipe coating and the field joint coating and avoid stress raisers due to geometric and material discontinuities. After the weld has been performed and passed inspection, an injection-moulded polypropylene (IMPP) field joint coating (FJC) is applied around the weld in order to replace the coating material that had been cut back prior to welding. The IMPP application process (described in more detail in Section 2.2) involves heating the steel to above 200°C. Since steel loses strength and stiffness with increasing temperature, the field joint is left to cool down so that the steel pipe can regain its strength and be bent to the reel without buckling or deforming excessively.

It is thus necessary to determine how long is required for the field joint to cool down sufficiently before reeling can take place safely. For field joints within a single stalk this is not an issue since the stalks are fabricated well in advance of reeling and so the field joints will have cooled down and regained full strength. However, during continuous reeling the stalks are joined together while the pipeline is being spooled with reeling paused while the weld is performed.

The pipeline is thus subject to barge motions and the associated fatigue effects which can further weaken the welds. It is advantageous that reeling is paused for a short time as possible so that allowances made for fatigue effects need not be too onerous; current best practice is to pause reeling at least overnight.

One of the primary factors dictating the cooldown time is the thickness of the insulating IMPP field joint coating, which can be controlled by using a specially-shaped mould for the IMPP, creating either hourglass or full FJCs (see Figure 3). A thinner coating allows for a quicker cooldown time and hence the strength of the steel is regained sooner. However, thicker FJCs contribute noticeably to the overall resistance of the field joint, even though the elastic stiffness and the strength of steel are orders of magnitude greater than those of the polymer coatings; although the steel yields at a strain of around 0.2% and loses much of its stiffness thereafter, the polymers

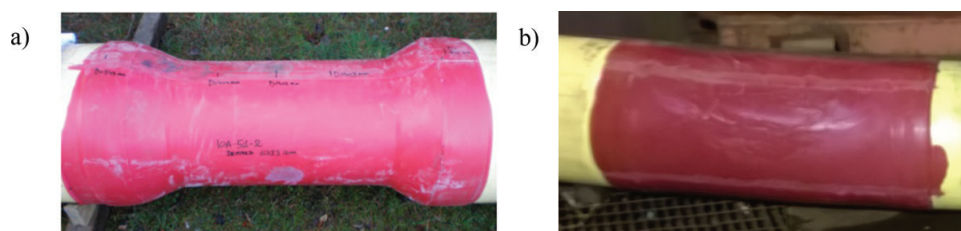


**Figure 3.** (a) Hourglass field joint coating; (b) full field joint coating.

maintain their elastic stiffness up to strains of approximately 2%, and thus contribute to the stability of the steel pipe when it is deforming plastically and help to prevent buckling. Thus, an optimal field joint coating thickness can be found where a balance is struck between steel strength being regained sooner and the contribution of the polymer material to the resistance of the joint.

In the current chapter, the experimental campaign is described and results presented, followed by a description of the thermal and mechanical numerical models developed to simulate the behaviour of the hot tie-in field joints. After successful validation of the models against the experimental results, a parametric study was conducted varying the thickness of the FJC and the cooldown time prior to bending, providing a matrix of viable coating and cooldown combinations upon which an appropriate operational envelope could be defined for the pipeline system.

## 2. Experimental investigation

Following successful qualification and commissioning of 12.75" pipelines with 53 mm-thick five-layer polypropylene (5LPP) coating for a previous project, it was initially decided to investigate the behaviour of a pipeline with 100 mm-thick nine-layer polypropylene (9LPP) coating in order to expand the reel-lay capacity envelope for the *Aegir*. Given that the inner radius of the reel is 8 m, the outer diameter of bare or thinly-coated reel-laid pipes is typically limited to 16" so that strains in the innermost layer of pipe around the reel are limited to 2.5% in accordance with DNV guidelines [5]. For thicker coatings, the strains in the outer surface of the coating increase accordingly, with a greater risk of damage to the pipe walls and coating. Thus, the primary aim of the experimental investigation was to assess whether these higher levels of strain could be withstood satisfactorily by the steel pipe and coating materials.

### 2.1. Specimens

Factory-coated test specimens were prepared comprising three pipe segments of grade X65 steel (yield strength  $f_y = 450 \text{ N/mm}^2$ ), with 20 mm girth-welded field joints. The field joints were 3.45 m apart in order to test two FJCs at the same time on the rig. The outer diameter of the pipes was nominally 327 mm, while the wall thickness was 15.7 mm, giving a diameter-to-thickness ratio of 20.8; the pipes were intentionally chosen to be this slender in order to provide a more onerous combination of pipe wall thickness and coating thickness [3]. The composition of the 9LPP coating is shown in **Figure 4**; after a thin three-layer polypropylene (3LPP) base layer is applied, alternating layers of foam and solid polypropylene are provided in order to combine the enhanced thermal insulating performance of the foam with the

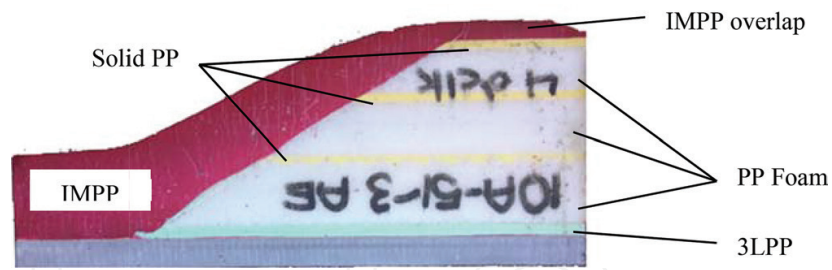


Figure 4. Chamfer section of 9LPP linepipe coating and IMPP field joint coating.

relative stiffness and strength of the solid polypropylene layers. Material fingerprinting was undertaken in parallel to the experimental investigation in order to characterise the thermal and mechanical properties of the various materials used in the pipeline system.

While the majority of specimens prepared were intended for full mechanical bend testing, a number of specimens were reserved in order to measure the heat evolution occurring within the liquid IMPP after injection. The temperatures were recorded using thermocouples, which were arranged as shown in **Figure 5**, in order to calibrate and validate thermal numerical models.

Three different FJC geometries were investigated: full, with a nominal thickness of 108 mm to include a 50 mm long, 8 mm thick overlap at the top of the chamfer, a thick hourglass with a nominal thickness of 50 mm, and a thin hourglass with a nominal thickness of 40 mm. A bare pipe with no FJCs was also tested in the bend rig as a control specimen. Temperature readings recorded by the thermocouples are presented and discussed in Section 3.2.3.

## 2.2. Setup and procedure

The tests were conducted at Heriot Watt University, Edinburgh, from November 2014 to January 2015. A coating station was installed onsite; for the specimens being used solely for temperature development measurement, the thermocouples were installed in the coating station also. The ambient temperature was recorded during each test.

The IMPP application process involves heating the bare steel substrate to temperatures around 240°C with an induction heater, then applying a thin layer of fusion bonded epoxy (FBE) followed by thin layers of chemically-modified polypropylene (CMPP) to encourage bonding between the steel substrate and the IMPP. The chamfers of the linepipe coating are reheated to encourage bonding with the IMPP, and a mould is then fitted around the field joint. The liquid polypropylene is then injected at 200°C into the mould, which is removed after some solidification of the polypropylene.

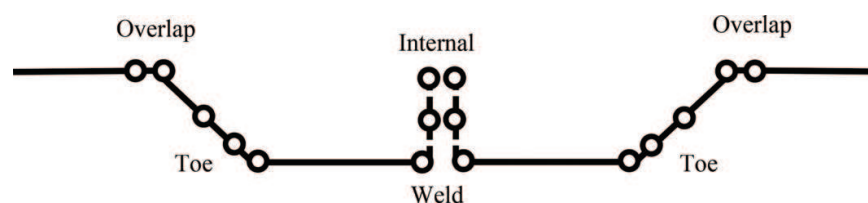
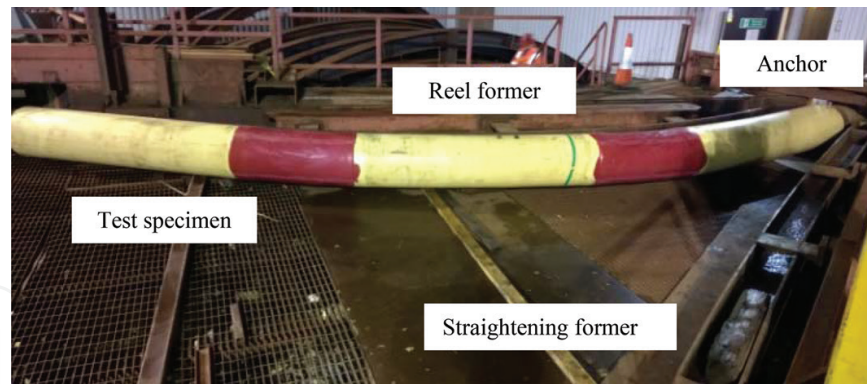


Figure 5. Schematic of thermocouple locations within the FJC.



**Figure 6.** Bend test rig at Heriot Watt University, with a test specimen bent to the reel former.

The bending rig consisted of a reel former with a radius of curvature equal to 8 m, and a straightening former with a radius of curvature equal to 55.84 m (see **Figure 6**); these radii are representative of those of the reel drum and straightener employed onboard DCV *Aegir*. After coating of the field joints was completed in the coating station, the pipe specimen was installed into the bending rig. One end of the pipe was anchored with a pin, while the other end of the pipe was attached to a pull head, which was translated between the two formers by means of a cable attached to a crane.

After a pre-defined cooldown period, the test procedure was initiated, whereby the specimen underwent five full bending cycles, with each cycle consisting of a number of steps: (i) the pipe is bent to the reel former and held; (ii) the pipe is released, (iii) the pipe is bent to the straightening former and (iv) the pipe is finally released again. The pipe was held to the reel former overnight in order to simulate the effect of the IMPP cooling down on the reel prior to resumption of reeling operations. The pipe is subjected to five full cycles during qualification testing in order to ensure that pipe integrity is maintained during initial spooling, straightening, bending over the aligner wheel and pipelay, along with contingencies for weather delays or the possibility of requiring to recover the pipe back onto the reel and then to unspool again. Ovality measurements were taken at salient locations after each cycle step, where the ovality is defined according to DNV design guidance [5] as:

$$\text{ovality} = (D_{\max} - D_{\min}) / (D_{\text{nom}}) \quad (1)$$

where  $D_{\max}$  is the maximum diameter of the deformed pipe,  $D_{\min}$  is the minimum diameter of the deformed pipe and  $D_{\text{nom}}$  is the original nominal diameter of the pipe. The ovality measurements were taken using optical metrology equipment inserted inside the pipe; thus, the values used in Eq. (1) relate to the inner diameter of the steel pipes with  $D_{\text{nom}} = 295.7$  mm.

### 3. Numerical modelling

Finite element modelling was used during the planning phase of the campaign in order to select suitable specimens, coating thicknesses and cooldown times for the tests; these models were refined further and validated against the experimental results. In the current section, the modelling techniques employed are described.

### 3.1. Modelling approach

In order to model the behaviour of the hot tie-in field joints, a thermo-mechanical model was required. Although coupled thermo-mechanical modelling is available in commercially-available finite element modelling software such as Abaqus [6], it is computationally expensive. An alternative approach employed in the current work is to separate the analysis into a thermal model to simulate the process of applying the IMPP, followed by a mechanical model simulating the process of bending the pipe that incorporates the temperature field predicted by the thermal model along with temperature-dependent material models.

Thermal modelling was performed using COMSOL Multiphysics [7], with the temperature fields around the field joint exported at a number of defined intervals of cooldown. These fields were then mapped onto an Abaqus mechanical model that simulated bend testing of the pipe. Given that the cooldown times are in the order of hours and that the bending events were performed in a number of minutes, there is a difference in orders of magnitude between the cooldown rates and the strain rate during the bend tests. Thus, it is reasonable to assume that heat flow within the field joints during bending was negligible and so can be accurately modelled by assuming a static temperature field in the mechanical models, thus achieving a considerable degree of efficiency over a fully-coupled thermo-mechanical model.

### 3.2. Thermal modelling

A time-dependent thermal model was developed in COMSOL Multiphysics, which was chosen due to its relative computational efficiency and modelling flexibility when compared to thermal modelling in comparable finite element modelling software. A section of the pipe around a particular field joint was represented by two-dimensional models assuming axisymmetric conditions about the longitudinal axis, with symmetry also assumed at the weld plane. The models relating to the three different FJC geometries are shown in **Figure 7**. It was found from sensitivity analysis that the change in temperature was negligible at a distance of 2 m from the weld, and thus the extent of the models reflects this. Triangular elements were used

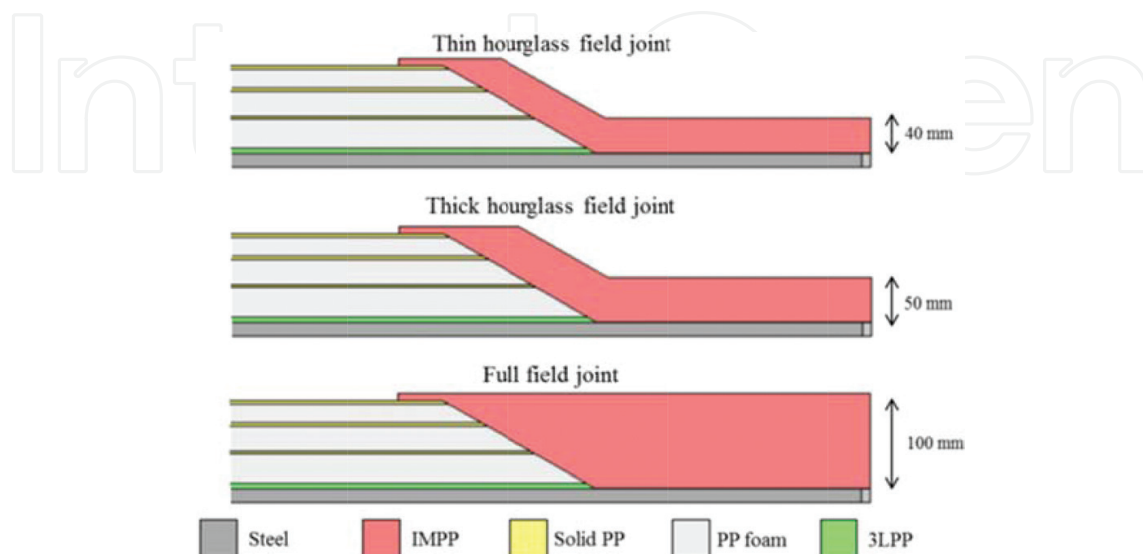


Figure 7. Modelling of field joints in COMSOL.



to mesh the model. Temperature-dependent thermal conductivities and heat capacities from an extensive campaign of material fingerprinting of coating materials and steel pipe materials conducted by Heerema Innovation were applied in the numerical models.

### 3.2.1. Boundary conditions

An air cooling boundary heat flux was imposed on external surfaces, with the convection transfer coefficient set equal to  $10 \text{ W/m}^2/\text{K}$ . When validating the numerical model against the experimental data, the ambient temperature was set equal to that recorded onsite on the day of testing; for the subsequent parametric study, the ambient temperature was set equal to  $20^\circ\text{C}$ .

Initially, it was assumed that internal airflow was negligible and so no boundary heat flux was defined along internal surfaces; this assumption is accurate for considerably long lengths of pipe where air flow is practically non-existent. However, for the shorter test specimens, the effects of internal air cooling on the temperature within the field joint coating are significant since heat is drawn from the polymer coating by the relatively highly-conductive steel pipe, which is being continually cooled by the air. It was found from sensitivity analysis that applying a temperature of  $18^\circ\text{C}$  and a heat transfer coefficient of  $3 \text{ W/m}^2/\text{K}$  along the internal surfaces of the models provided appropriate cooldown rates.

### 3.2.2. Analysis steps

The analysis was divided into a number of steps representing the IMPP application procedure as conducted onsite. Firstly, induction heating of the steel was modelled using a body heat flux defined appropriately to raise the temperature of the steel pipe to  $240^\circ\text{C}$  within the recorded operating time. Next, domains representing the layers of FBE and CMPP were added to the model and the analysis was resumed in order to simulate cooling of the steel substrate to  $190^\circ\text{C}$ . Reheating of the chamfers was simulated by applying a surface heat flux to the relevant surfaces in the model, defined appropriately so as to replicate reheating to between  $140$  and  $150^\circ\text{C}$  during the time recorded onsite.

In the final step of the thermal analysis, the IMPP was included at an initial temperature of  $200^\circ\text{C}$ . The model was run to simulate 16 h of cooldown to provide comparison with the thermocouple data. Three separate models were created for the full, thick hourglass and thin hourglass FJC geometries, respectively, as shown in **Figure 7**.

### 3.2.3. Validation of thermal model

The temperature evolution profiles recorded by the thermocouples (located at the positions indicated in **Figure 5**) for the thick hourglass FJC specimen are shown in **Figure 8** as solid lines. It can be seen that, as would be expected, temperatures recorded closer to the outer surface of the FJCs at the overlap reduce quicker than those located internally. Owing to thermal conduction through the steel pipe, the temperatures at the weld and toe locations reduce quicker than at the internal thermocouples where the insulating polymer slows down heat flow considerably. This effect was noticeably more pronounced in the full FJC than in the hourglass FJCs, with the temperature reducing quickest in the thin hourglass FJC.

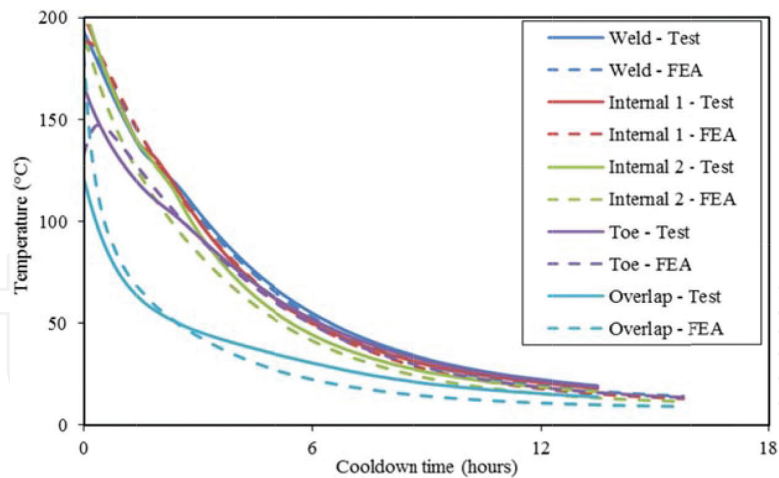


**Figure 8.** Experimental and numerical temperature evolutions for the thick hourglass FJC specimen.

The predictions of the numerical models are shown as dashed lines in **Figure 8**. Good agreement is observed between the experimental observations and the numerical predictions, particularly at the weld and toe locations and also at the internal thermocouples, while some discrepancy is observed to develop at the external overlap locations; this behaviour was also observed in the full FJC and thin hourglass FJC models. This can most likely be attributed to the overestimation of the convection transfer coefficient for the external boundary cooling coefficients. It is noticeable that since this discrepancy is more prevalent on the external boundaries rather than in the rest of the model, the majority of temperature loss in the IMPP is due to conduction through the steel, rather than from air convection. Overall, the accuracy of the numerical predictions is confirmation of the suitability of the modelling techniques and the material models used, and allows for the temperature fields to be applied to the mechanical models in the next stage of the analysis.

### 3.3. Mechanical modelling

Modelling of the bend test procedure was performed using Abaqus 6.12 [6]. For validation of the model, the measured geometry of the test specimens was used, while for the parametric study, nominal dimensions were used. Temperature-dependent material models were used in the simulations as outlined in Section 3.3.2, with the temperature fields predicted by the thermal modelling mapped to the Abaqus models using the procedure outlined in Section 3.3.4. The model was validated successfully against the experimental results for ovality and stress distributions, which then allowed a parametric study to be conducted to identify combinations of FJC thickness and cooldown time where buckling is avoided.

#### 3.3.1. Model geometry and boundary conditions

The model of the bend test rig is shown in **Figure 9**, with a combination of shell and solid instances used to model the pipe and coating materials, with two FJCs centred at 20 mm girth welds. A pipe with no FJCs was also modelled in order to provide validation against the bare pipe tested onsite.

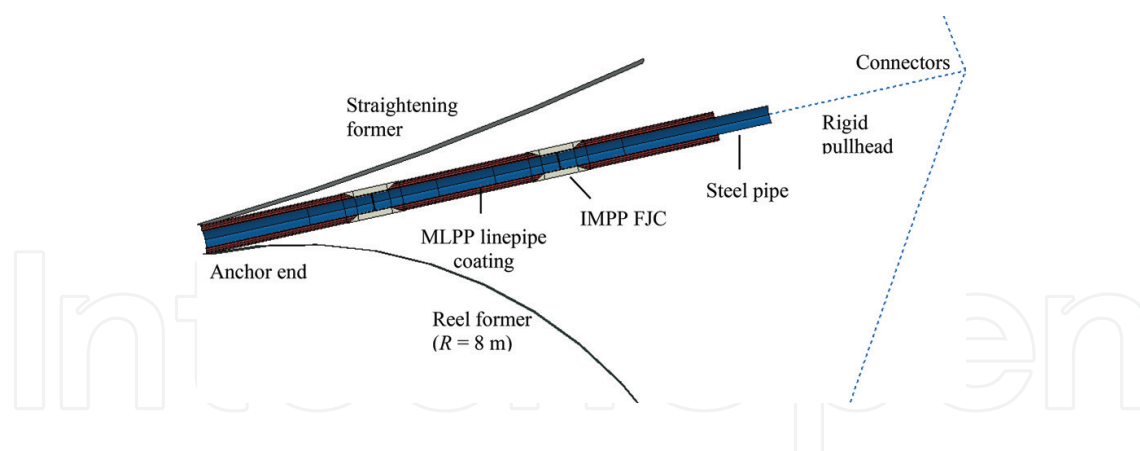


**Figure 9.** Model of the bend test rig and pipe specimen in Abaqus.

Analytical rigid instances were used to model the reel former and straightening former, each with a radius of curvature equivalent to those used onsite, respectively. Pin-ended conditions were defined at the anchor end, permitting only rotation in the plane of the rig. Connector elements were used to model the cables from the pullhead to the crane with appropriate displacements imposed on them in order to simulate the pipe being bent to the formers across the various analysis steps.

Contact interactions were defined between the outer surface of the coating and the former surfaces, with a coefficient of friction of 0.3 to define the tangential behaviour and a pressure overclosure to define the normal behaviour.

### 3.3.2. Material modelling

As part of a campaign of material fingerprinting conducted by Heerema Marine Contractors, moduli of elasticity and full stress-strain curves for the various polymer and steel materials used in the pipes were obtained at a number of ambient temperatures and strain rates. A typical set of stress-strain curves is shown in **Figure 10** for the IMPP material, with testing performed at 5 mm/min; these curves were converted to true stress and true strain prior to their use in the numerical models. For temperatures outside the tested range, the material curves were based on extrapolation. For the polypropylene materials, an elastic-plastic material model with isotropic hardening was assumed, in keeping with previous studies [8]. Although polypropylene exhibits viscoelastic behaviour in practice, given the strain rates and hold times being modelled in the current study, it was not necessary to model changes in stress owing to viscous flow of the material.

The moduli of elasticity of the various coating materials were modelled as temperature-dependent, while the Poisson's ratio was set at 0.45. The coefficient of thermal expansion for the three polypropylene materials was temperature-dependent and based on manufacturers' recommendations.

The X65 material was also modelled using an elastic-plastic material model albeit with non-linear kinematic hardening, and based on test data obtained across a range of temperatures. For temperatures outside the tested range, material curves were extrapolated based on derating the material in accordance with DNV guidelines [5]. The resulting true stress-true strain curves are shown in **Figure 11**. The stress-strain relationship for the welds was assumed to be similar to that of the parent steel, albeit with isotropic hardening and a strength overmatch of

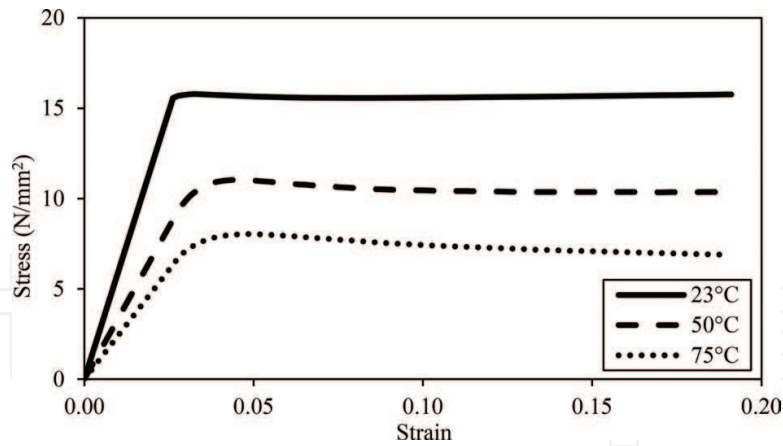


Figure 10. Stress-strain curves for the IMPP material obtained from tensile testing.

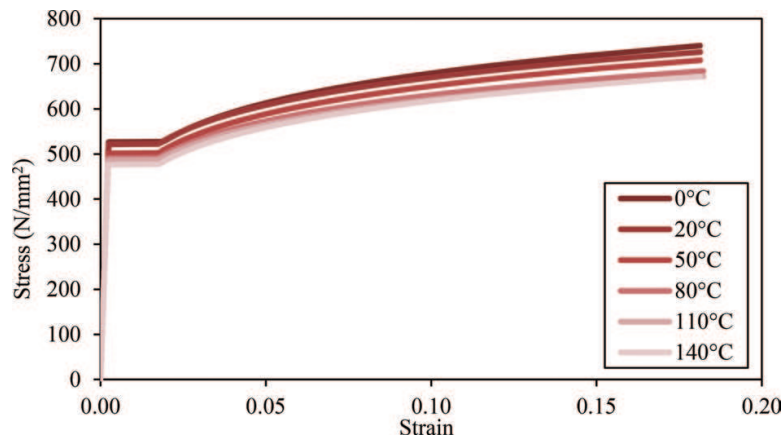


Figure 11. Stress-strain curves for X65 steel at a range of temperatures.

80 N/mm<sup>2</sup> based on previous project experience. The modulus of elasticity of the steel materials was assumed to be 210,000 N/mm<sup>2</sup> with a Poisson's ratio equal to 0.3. The coefficient of linear expansion was set equal to  $13 \times 10^{-6}$ .

### 3.3.3. Elements and meshing

In the interests of computational efficiency, the mechanical model employed a combination of quadrilateral shell S4R elements for the steel pipe, and solid C3D8R elements for the thicker coating materials. The steel pipe elements were in fact composite layups in order to include the thin layers of FBE and CMPP. A nominal element size of 15 mm was used, with the mesh density increased in the area of interest around the weld.

### 3.3.4. Mapping of temperature fields

The thermal analysis was performed using two-dimensional axisymmetric models with triangular meshes, while the mechanical analysis used three-dimensional solid brick and quadrilateral shell elements. In order to map the temperature field correctly, an algorithm was developed whereby the COMSOL temperature field was centred on a weld plane and then

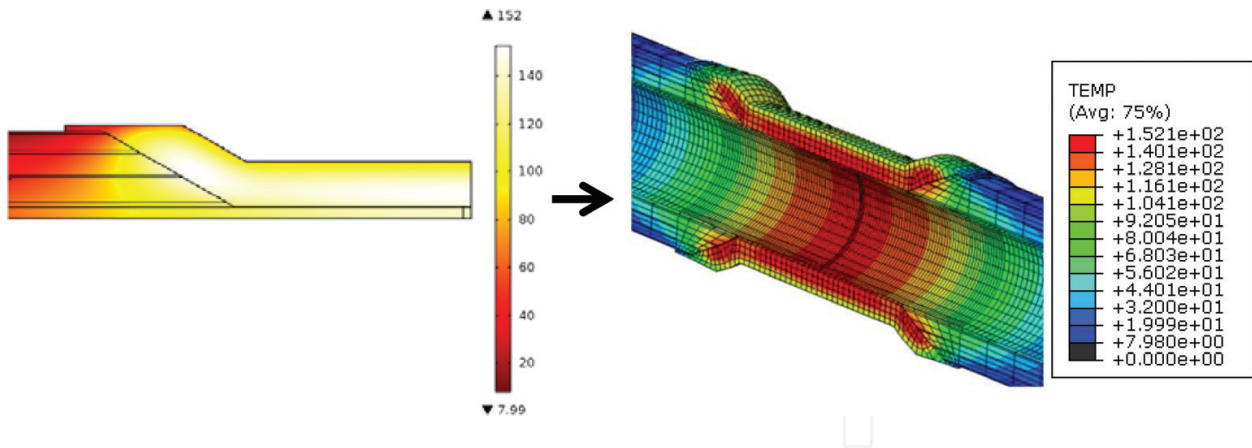


Figure 12. Example of transferral of COMSOL temperature output to a discrete field in Abaqus.

translated and rotated to cylindrical coordinates. A least-squares node-matching routine then identified the nodes in the COMSOL mesh closest to each node in the Abaqus mesh within longitudinal neighbourhoods of 100 mm. The resulting field was then inputted as a discrete field into the Abaqus model. An example of the result of running the algorithm is shown in **Figure 12**, with the COMSOL temperature output on the left hand side and the resulting temperature field in Abaqus shown on the right. For the validation of the numerical models against the experiments, temperature fields were outputted at the appropriate cooldown times related to the time after IMPP application recorded during the bend tests. Since there was a half hour to an hour difference in application time between the two FJCs for a particular test pipe, and thus a noticeable difference in temperature, separate temperature fields were mapped around the two joints.

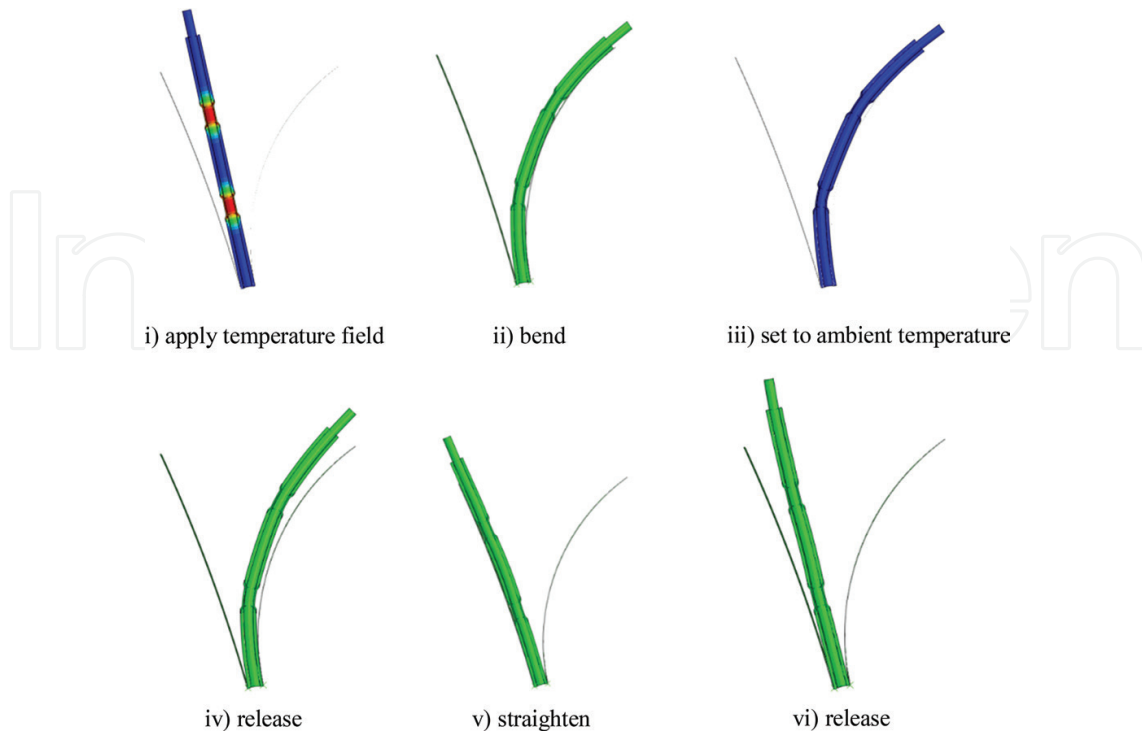


Figure 13. Bend cycle steps modelled in Abaqus.

### 3.3.5. Analysis procedure

A geometrically-nonlinear static analysis was employed, divided into a number of steps, as shown in **Figure 13**: (i) firstly, the temperature field was applied to the model; (ii) next the pipe was bent to the reel former and held; (iii) the temperature field was then set equal to the appropriate ambient temperature (either that recorded onsite for the validation study, or 20°C for the parametric study) in order to simulate the pipe and FJCs cooling down; (iv) next, the pipe was released, then (v) bent to the straightening former, and finally (vi) released again, thus completing the first bend cycle. The model simulated five full bending cycles in total (the latter four all with the temperature field set equal to the appropriate ambient temperature). As can be seen in **Figure 13**, after a full bend cycle there is a noticeable amount of plastic deformation present in the pipe after straightening; limiting this plastic deformation and avoiding buckling of the pipe and tearing of the coating are two of the main challenges posed by the reel-lay procedure.

## 4. Results and comparisons

In this section, the results of the bend tests are discussed, and comparison is made with the predictions of the numerical model.

### 4.1. Pipe deformation, buckling and ovality

A bare pipe with no FJCs was tested first in the bend rig as a control specimen, whereupon it buckled at the first bend to the reel former, as shown in **Figure 14a**; this early onset buckle can be attributed to the stiffness mismatch between the full linepipe coating and the bare steel pipe causing strains to concentrate within the bare steel. It can also be seen that the point of initiation of the buckle is located to the left of the weld. The strain field predicted by the numerical model is shown in **Figure 14b**, where the strain concentration can indeed be observed in the uncoated region of the pipe. It can be seen that the pipe was also predicted to buckle after the first bend to the reel, albeit with the point of initiation of the buckle located closer to the weld. Given the high imperfection sensitivity of cylindrical shells in compression, this discrepancy in buckle location is likely down to a localised thinning of the pipe wall in the area around the buckle due to corrosion. It can be seen that, in areas in the steel pipe away from the buckle, the tensile strain is approximately 2.5%, in keeping with analytical predictions.

Despite the presence of the polymer coating, one of the field joints on the pipe with the thin hourglass FJC also buckled on the first bend to the reel. During initial simulations prior to the test campaign, ovalities in excess of 10% were expected; based on previous experience [9] this level of ovality is a strong predictor of the occurrence of buckling. The buckled field joint is shown in **Figure 15a**; as can be seen, there is noticeable lift-off from the reel former. In **Figure 15b**, the equivalent numerical prediction of the stress field is shown, with rippling observable in the compression zone.

The pipes with the thick hourglass and full FJCs did not buckle throughout the five bending cycles; the numerical models also predicted that no buckling would occur. In **Figure 16**, the ovalities recorded along the length of the pipe with the thick hourglass FJC after the first bend

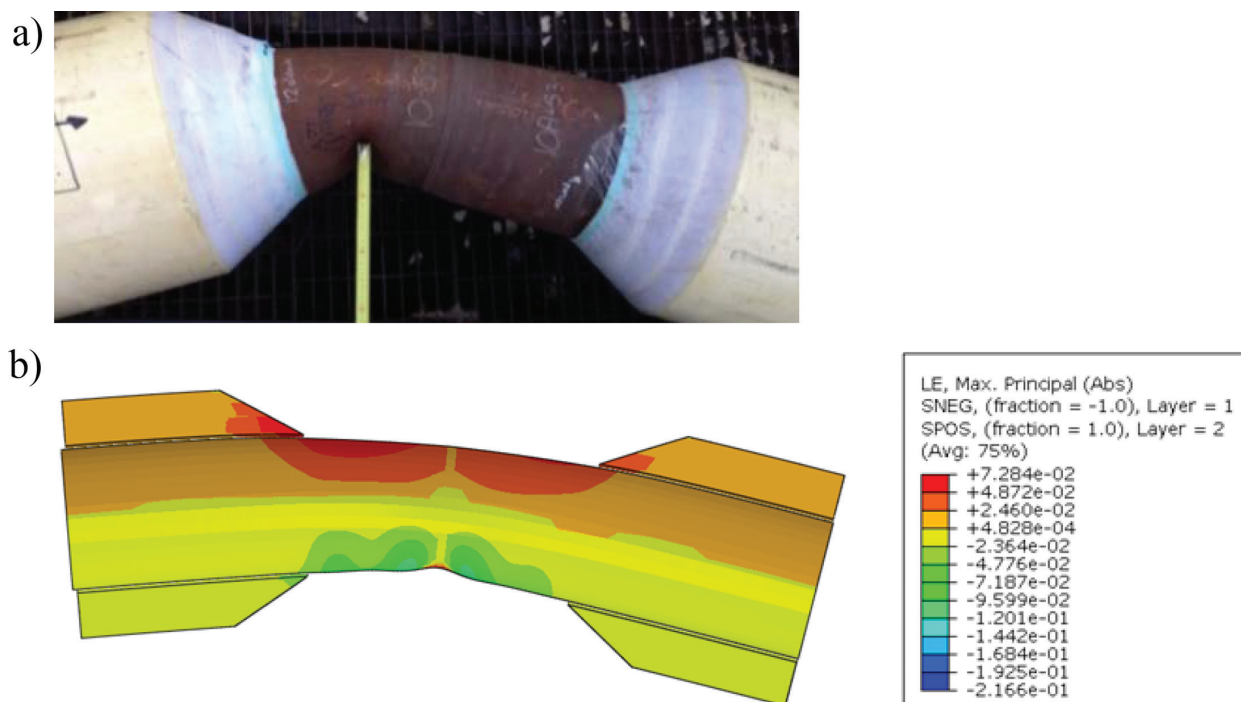


**Figure 14.** Bending of field joint with no coating; (a) experimental observation and (b) numerical prediction of strain field.

to the reel are compared with numerical predictions, with the ovalities calculated using Eq.(1). The two peaks in the ovality distributions coincide with the location of the field joints. As can be seen, there is particularly good agreement in the region around the field joint furthest from the anchor end, while the predictions of ovality are underestimated at the field joint closest to the anchor end. This can be attributed to some relaxation of contact stress towards the anchor end during the simulation as the point of contact progresses along the pipe. Similar accuracy was obtained across all the tested pipes, thus increasing confidence in the ability of the numerical model to predict pipe deformations and ovalities but most importantly whether the field joints can withstand five full bending cycles without buckling. The results of the experimental investigations and the numerical analysis showed that, provided the correct FJC thickness is applied, reeling of pipelines with 100 mm-thick MLPP coatings is indeed achievable.

#### 4.2. Stress whitening

During testing of the specimens with FJCs applied, a phenomenon known as stress whitening was observed. Stress whitening occurs when the molecule chains within a polymer become damaged due to excessive tensile stresses causing plastic deformation, with holes and tears forming as the molecular structures are altered [10]. Light incident upon the affected zones is then diffused and scattered more readily, appearing as white discolorations on the surface of the polypropylene. In the following discussion, comparisons are made after the first bend to the reel former and holding in position overnight, i.e., after the field joint has cooled down fully.

Owing to the inherent difficulty of installing stress measuring instrumentation into the coating and retrieving it afterwards, visual identification of stress whitening was used as an indicator of tensile stress concentrations within the IMPP material. In **Figure 17**, the appearance

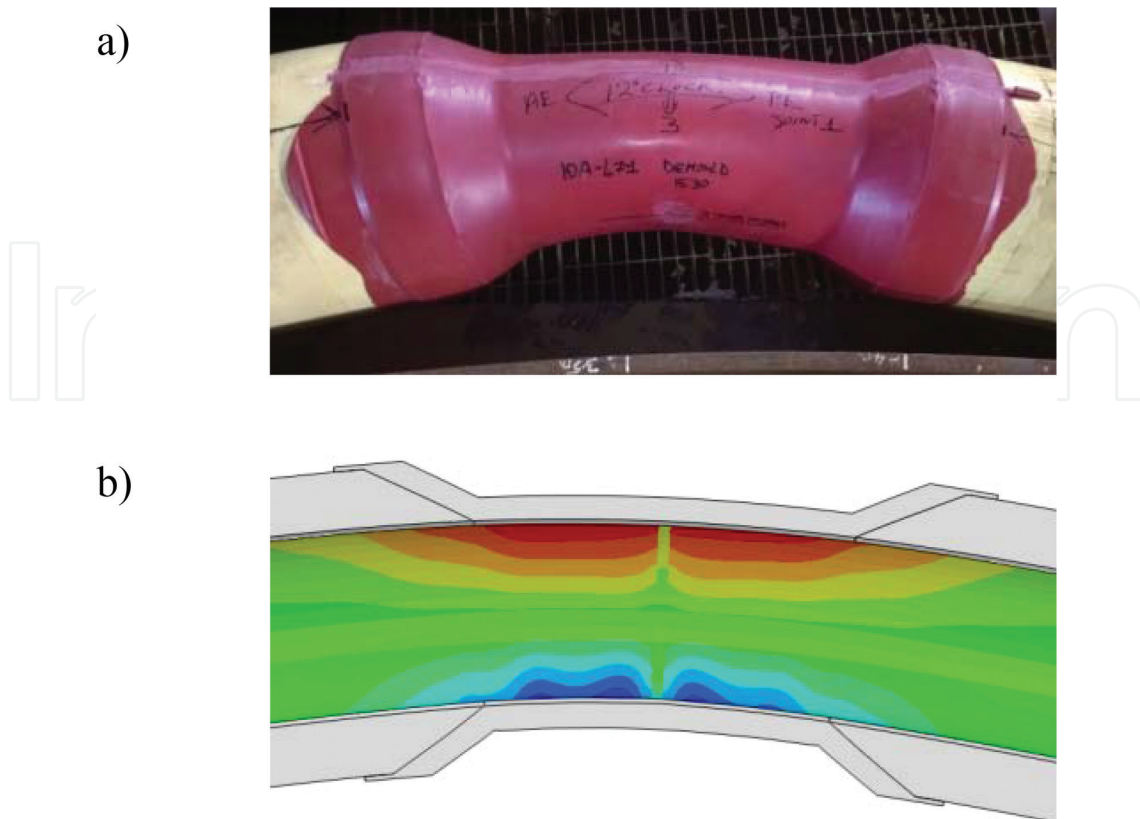


Figure 15. Pipe with thin hourglass FJC; (a) experimental observation, (b) simulated stress field with rippling observable.

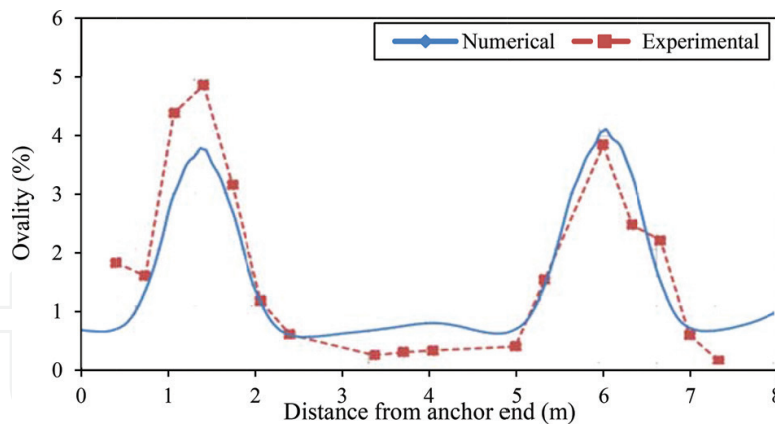


Figure 16. Comparison of measured and predicted ovality distributions in the pipe with the thick hourglass FJCs after the first bend to the reel.

of stress whitening in the thick hourglass FJC is compared to the numerical prediction of the principal stress field. Given that the yield stress is approximately  $16 \text{ N/mm}^2$  it can be seen that the location of areas where plastic deformation has occurred agree very well with the location of stress whitening above the chamfer toes observed onsite.

In the case of the thin hourglass FJC, as can be seen in Figure 18a, the level of stress whitening was not as prevalent or as noticeable, indicating that much less plastic deformation has occurred than in the thick hourglass FJC. This corroborates with the predicted stress field



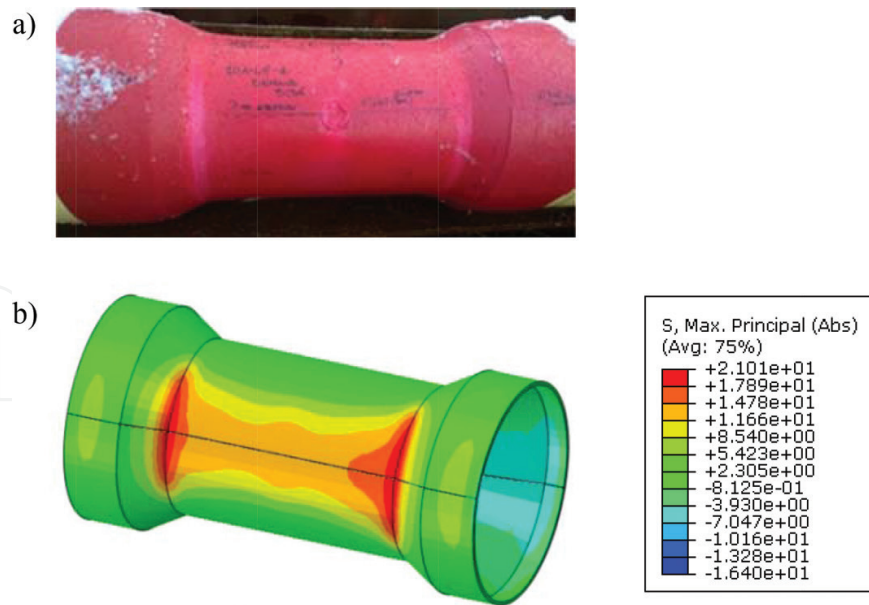


Figure 17. Thick hourglass FJC; comparison of (a) stress whitening observed during test with (b) numerical prediction of stress.

shown in **Figure 18b** where the maximum stress is  $13.85 \text{ N/mm}^2$ , suggesting that the material has not yielded yet (although in practice some polymer chains may have been damaged already when the material was hotter and therefore less strong, as evidenced by the material curves shown in **Figure 10**). While it may be counter-intuitive that less stress whitening has occurred in the thin hourglass FJC rather than in the thick hourglass FJC, this can be explained by considering the reduction in longitudinal strain on the outer surface of the thin hourglass FJC since it is closer to the neutral axis of the section than the outer surface of the thick hourglass FJC. It can be seen that the areas of peak stress above the chamfer toe coincide with the lightest areas on the external surface of the tested pipe.

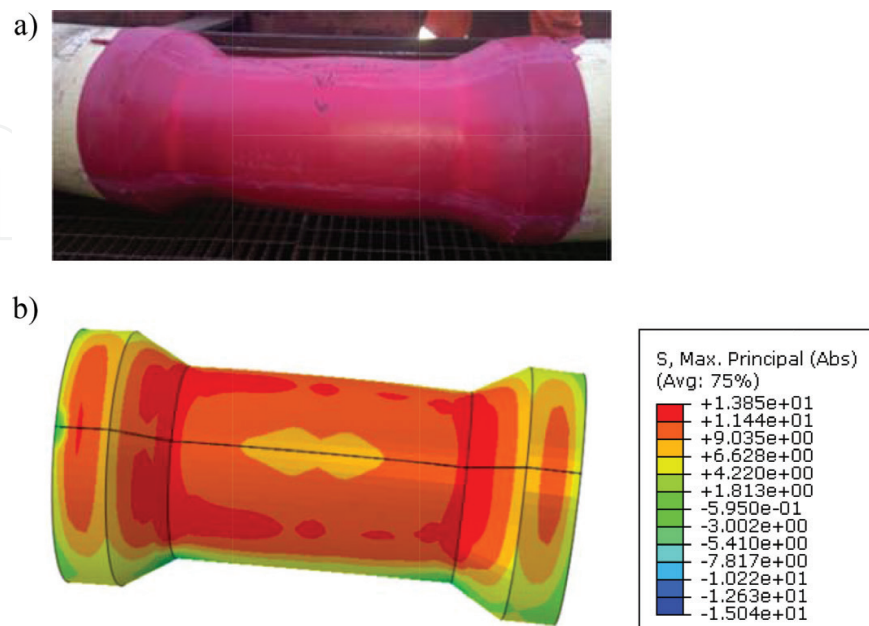


Figure 18. Thin hourglass FJC; comparison of (a) stress whitening observed during test with (b) numerical prediction of stress.

In the full FJC, stress whitening was observed after testing as shown in **Figure 19a**; stress concentrations were also predicted in the numerical model above the chamfers, as shown in **Figure 19b**. Although the agreement is not as clearly observable as in the hourglass FJCs, the level of stress predicted in the areas of stress whitening is commensurate with the yield stress of the material.

Finally, in addition to the three pipes with hot tie-in field joints, another pipe with full FJCs was tested after it had fully cooled down to the ambient temperature. As can be seen in **Figure 20a**, there was no evidence of stress whitening visible in this specimen, and as shown in **Figure 20b**, the numerical model also predicted a uniform stress field with no concentrations, with maximum stresses of approximately 15 N/mm<sup>2</sup> in the IMPP.

Bending of the steel when it is still hot and weakened leads to higher strains and deformations around the field joint as a whole. The thin hourglass field joint would have cooled quicker than the thick hourglass field joint, allowing the steel to regain relatively more strength and thus limiting the amount of strain. The increased deformation in the thick field joint has led to higher stresses in the pipe as well as the field joint coating, which can be observed upon comparison of **Figures 17b** and **18b**.

In the each of the three hot tie-in field joints, it can be seen that stress concentrations and areas of stress whitening occur above the chamfers, particularly above the chamfer toe. One explanation is that there is a stiffness mismatch either side of the chamfer that causes stress to accumulate at this point; however, the transition between the IMPP field joint coating and the MLPP linepipe coating occurs quite gradually over the length of the chamfer (approximately 175 mm), and so sudden peaks in stress would not be expected. Upon inspection of the evolution of the distribution of ovality along the length of the pipe specimens during the bend test, a correlation between the ovality gradient and the peaks in stress was apparent. In **Figure 21**, the distribution of ovality gradient along the length of the thick hourglass FJC specimen, as predicted by the numerical model, is shown. The locations of the chamfers and field joints are also overlaid on the graph. It can be seen that areas of peak ovality gradient coincide with the toes of the chamfer, where

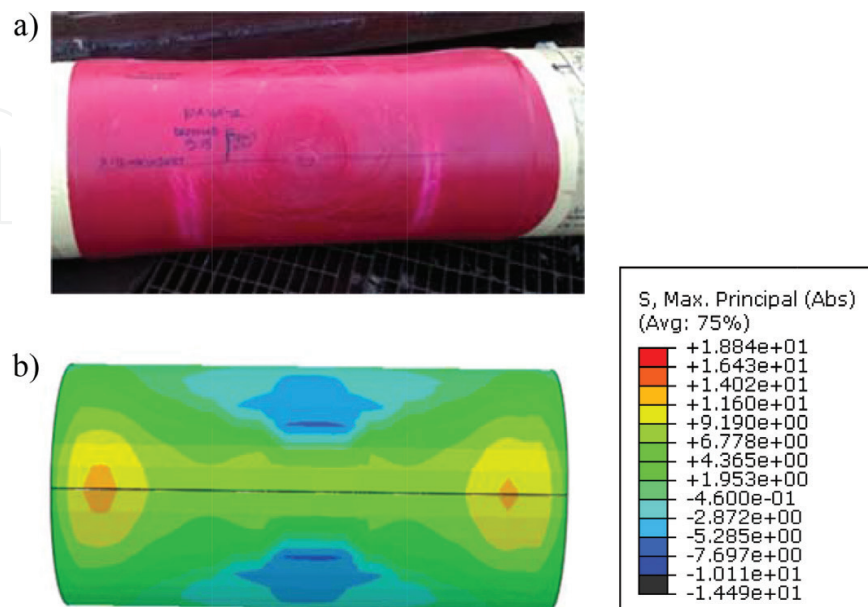


**Figure 19.** Full hourglass FJC; comparison of (a) stress whitening observed during test with (b) numerical prediction of stress.

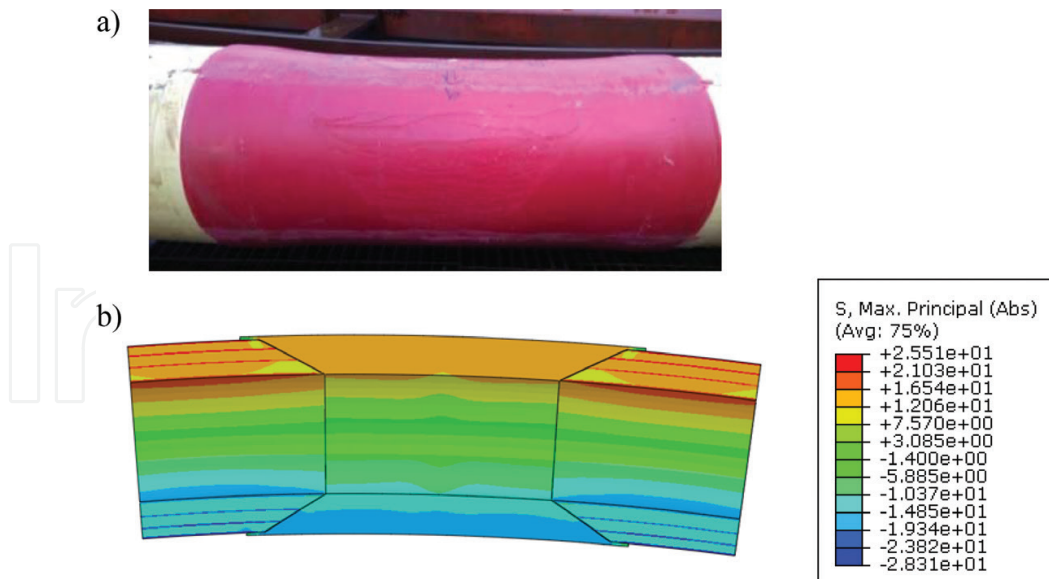


**Figure 20.** Full hourglass FJC bent after being fully cooled down; comparison of (a) stress whitening observed during test with (b) numerical prediction of stress.

stress whitening was also observed very clearly in the test pipe, as shown in **Figure 17a**. In addition, although stresses close to yield were predicted by the numerical model in the full FJCs of the pipe that was bent after fully cooling down, since the stress distribution and also ovality distribution were quite uniform, i.e., with a small gradient, there was no stress whitening visible. This agreement between peak ovality gradient and areas of stress whitening can be attributed to the higher levels of strain associated with sudden large deformations in the steel pipe, which would cause associated large strains, and hence stresses, in the coating materials.

### 4.3. Parametric study

As demonstrated by the comparisons between the experimental observations and the numerical results, the thermal and mechanical models are capable of accurately predicting the behaviour of hot tie-in field joints in bending. With the model validated, a parametric study was conducted

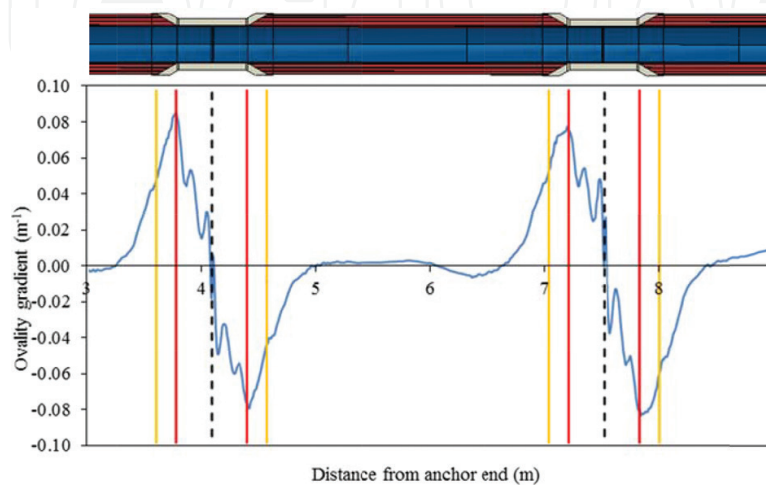


**Figure 21.** Ovality gradient along the length of the pipe with the thick hourglass FJC with chamfer locations overlain.

varying the thickness of the FJCs and the amount of cooldown time. Bend tests on pipes with FJC thicknesses from 20 mm up to a full FJC and cooldown times from 1 hour up to 24 hours were simulated and assessed to ascertain whether five full bend cycles could be completed without the pipe buckling. The results of the parametric study showed that an optimal thickness and cooldown time existed that represented significant material and time savings compared to current practice.

## 5. Conclusions

Finite element models simulating the thermal and mechanical behaviour of hot tie-in field joints during coating application and bending have been developed. Experimental investigations recording the temperature evolution profiles within the field joint coatings after pouring and the mechanical behaviour of the field joints during bend testing were used as a basis for calibration and validation of the numerical models. Three separate field joint coating geometries were tested in order to examine the influence of coating thickness on the overall behaviour of the field joint.

Thermal modelling in COMSOL Multiphysics employed temperature-dependent thermal properties obtained from material fingerprinting. It was found that it was necessary to model internal air cooling in the test specimens, which would not normally be required when modelling longer pipeline sections. Close agreement was observed upon comparison of temperature evolutions recorded onsite with those predicted by the numerical models, allowing for the predicted temperature fields to be subsequently applied to mechanical models.

Numerical models were developed in Abaqus to simulate bend testing of the various pipe specimens, employing temperature-dependent material models obtained from material fingerprinting. Temperature fields obtained from the thermal numerical models were mapped onto the mechanical models and the process of bend testing over five full bend cycles simulated. The numerical predictions for pipe ovality and coating stress distributions were compared with the experimental results, with close agreement observed. It was also found that ovality gradient can be used as a predictor of the occurrence of stress whitening in the coating materials. The numerical analysis, coupled with the results of the experimental investigation, showed that reeling of pipes with 100 mm-thick coating is possible.

The successful validation of the numerical models allowed for an extensive parametric study to be conducted, varying the field joint coating thickness and the cooldown times provided after application of the IMPP. It was found that an optimal FJC thickness existed that balanced the quicker cooldown times associated with thinner FJCs with the material strength benefits of thicker FJCs. The results of the study showed that use of this optimal FJC thickness can result in significant time savings when conducting reeling operations in practice.

## Acknowledgements

The authors wish to thank the team at the Innovation Department of Heerema Marine Contractors for their assistance during the planning and execution of the experimental campaign, and also to David Haldane and the technical staff at Heriot Watt University for their support throughout testing.

## Author details

Finian McCann<sup>1\*</sup>, Guido Ridolfi<sup>2</sup>, Erwan Karjadi<sup>2</sup>, Harm Demmink<sup>2</sup> and Helen Boyd<sup>2</sup>

\*Address all correspondence to: [mccannf@lsbu.ac.uk](mailto:mccannf@lsbu.ac.uk)

1 School of the Built Environment and Architecture, London South Bank University, UK

2 Heerema Marine Contractors, Netherlands

## References

- [1] Smith SN, Clough T. Deepwater pipeline installation by reel-lay method. In: Proceedings of the Offshore Technology Conference 2010, 3-6 May 2010, Houston, TX; 2010
- [2] Karjadi E, Boyd H, van Rooijen R, Demmink H, Balder T. Development of Aegir reeling pipeline analyses by test validation. In: Proceedings of the 32nd International Conference on Ocean, Offshore and Arctic Engineering, 9-14 June 2013, Nantes, France; 2013
- [3] Ridolfi G, Boyd H, Karjadi E, Demmink H, McCann F, de Bode A. Extension of the reel-ability envelope of the Aegir: synergy between analysis and full-scale testing. In: Proceedings of the 25th International Ocean and Polar Engineering Conference, 21-26 June 2015, Hawaii, USA; 2015
- [4] Crome T. Reeling of pipelines with thick insulation coating: finite-element analysis of local buckling. In: Proceedings of the Offshore Technology Conference 1999, 3-6 May 1999, Houston, TX; 1999
- [5] Det Norske Veritas. DNV-OS-F101: Submarine Pipeline Systems. DNV. 2013. Vol. 2013
- [6] Abaqus. 2012. ABAQUS analysis user's manual, v6.12.3. USA: Dassault Systems Simulia Corp., Providence; 2012
- [7] COMSOL, Inc. COMSOL Multiphysics 4.2a. COMSOL, Inc. 2011; 2011
- [8] Karjadi E, Boyd H, Demmink H, Thibaux P. Reeling pipeline material characterization – testing, material modeling and offshore measurement validation. In: Proceedings of the 34th International Conference on Ocean, Offshore and Arctic Engineering, 31 May–5 June 2015, St. Johns, Canada; 2015
- [9] Karjadi E, Boyd H, van Rooijen R, Demmink H, Balder T. Development on Aegir reeling pipeline analyses by test validation. In: Proceedings of the 32nd International Conference on Ocean, Offshore and Arctic Engineering, 9-14 June 2013, Nantes, France; 2013
- [10] Pae KD, Chu H-C, Lee JK, Kim J-H. Healing of stress-whitening in polyethylene and polypropylene at or below room temperature. *Polymer Engineering & Science*. 2000;**40**(8): 1783-1795